



## Enhanced Extraction and Efficiency of Blue Light-Emitting Diodes Prepared Using Two-Step-Etched Patterned Sapphire Substrates

Ray-Ming Lin,<sup>a,b,\*</sup> Yuan-Chieh Lu,<sup>a</sup> Sheng-Fu Yu,<sup>c</sup> Yew-Chung Sermon Wu,<sup>d</sup>  
Chung-Hao Chiang,<sup>a</sup> Wen-Ching Hsu,<sup>e</sup> and Shoou-Jinn Chang<sup>c,\*</sup>

<sup>a</sup>Department of Electronic Engineering and <sup>b</sup>Green Research Technology Center, Chang-Gung University, Taoyuan 333, Taiwan

<sup>c</sup>Institute of Microelectronics and Department of Electrical Engineering, Center for Micro/Nano Science and Technology Advanced Optoelectronic Technology Center, National Cheng-Kung University, Tainan 70101, Taiwan

<sup>d</sup>Department of Materials Science and Engineering, National Chiao-Tung University, Hsinchu 300, Taiwan  
<sup>e</sup>Sino-American Silicon Products Incorporated, Hsinchu 300, Taiwan

Using a hot acid wet etching method, we have fabricated two types of patterned sapphire substrates: A pyramidal patterned sapphire substrate (PPSS) and a flat-top patterned sapphire substrate (FTPSS). After placing these samples into an atmospheric pressure metallorganic chemical vapor deposition system, we deposited standard InGaN light-emitting diode (LED) structures onto their surfaces. The crystal quality of these two surfaces was enhanced, as evidenced using X-ray diffraction (the full width at half-maximum decreased from 406.8 arcsec for the conventional sapphire to 356.4 and 349.2 arcsec for the PPSS and FTPSS samples, respectively). The output power of InGaN-based blue LEDs incorporating the PPSS and FTPSS improved to 17.9 and 18.7%, respectively, at 20 mA.

© 2009 The Electrochemical Society. [DOI: 10.1149/1.3231502] All rights reserved.

Manuscript submitted May 26, 2009; revised manuscript received August 3, 2009. Published October 1, 2009.

Gallium nitride (GaN)-based light-emitting diodes (LEDs) have attracted much attention in recent years because of their high performance and promising reliability.<sup>1,2</sup> They are also considered to be one of the best candidates for replacing conventional incandescent and fluorescent lamps. Many commercial applications of GaN-based LEDs have been realized: e.g., traffic signals, large-scale full-color outdoor displays, backlighting of liquid crystal displays, and cell phones. Although GaN-based LEDs have great potential for use in solid-state lighting, the output efficiency remains limited because of many dislocations within the structures that result from the large lattice mismatch and the different thermal expansion coefficients of the sapphire substrate and GaN. Because the threading dislocation density (TDD) is usually ca.  $10^7$ – $10^9$  cm<sup>-2</sup> in a grown GaN film,<sup>3</sup> GaN LEDs usually exhibit greatly reduced internal quantum efficiencies (IQEs).

Epitaxial lateral overgrowth (ELOG) is one method proposed to overcome the problem of dislocation in GaN epitaxial films.<sup>4,6</sup> First, a thin GaN buffer layer is grown on top of the sapphire substrate, and then a striped SiO<sub>2</sub> mask is deposited onto the buffer layer. Device epitaxy is then performed following the preparation of the mask. The presence of the SiO<sub>2</sub> mask causes dislocation stretching from the sapphire–GaN interface to be blocked, thereby creating a nearly dislocation-free region in the GaN film, and thereby reducing the TDD by about 2 orders of magnitude. Though ELOG is good at reducing the TDD, the two-step growth procedure is rather complicated and can lead to reactor contamination. To reduce the complexity of ELOG, a maskless and single-step growth method using a patterned sapphire substrate (PSS) has been proposed. In the early stages of PSS development, the patterns were created using dry etching techniques (e.g., inductively coupled plasma reactive ion etching), which could cause surface damage and result in a poor quality epilayer–substrate interface. More recently, wet etched PSSs have attracted more attention because of their higher production yields, lower cost, and smoother surfaces. The use of a PSS not only increases the IQEs of the LEDs but also improves the light extraction efficiency because of the nonplanar interface between the sapphire substrate and the GaN film. In this study, we prepared PSSs having two types of surface morphology: A pyramidal patterned

sapphire substrate (PPSS) and a flat-top patterned sapphire substrate (FTPSS), and grew InGaN-based LEDs on top of them. We measured the electrical and optical properties to verify the output enhancement effects of the PPSS and FTPSS and determined the internal residual strain effect.

LEDs were grown on PSS samples possessing convex pyramid and flat-top formation arrays, respectively. The optical and electrical properties of these two samples were compared with those of an LED grown on a conventional planar sapphire. First, a 2400 Å thick layer of SiO<sub>2</sub> was deposited on top of the original sapphire substrates using plasma-enhanced chemical vapor deposition for use as an etching mask. An 8000 Å thick SiO<sub>2</sub> film was also applied on the back of the sapphire substrate to avoid back-side roughening while processing the surface pattern. The basic photoresist hexagonal arrays of the PPSS and FTPSS were defined photolithographically. After forming the patterned SiO<sub>2</sub> mask, the samples were dipped into a mixture of 98 wt % H<sub>2</sub>SO<sub>4</sub> and 68 wt % H<sub>3</sub>PO<sub>4</sub> (3:1 v/v) at 280°C to create the convex FTPSS.<sup>7,8</sup> A two-step wet etching method, which had not been widely studied, was sequentially used to make the PPSS: (i) The FTPSS sample created in the first step was again immersed in a buffered oxide etch solution to remove all SiO<sub>2</sub> masks and (ii) the FTPSS sample without the SiO<sub>2</sub> cap was dipped into the hot acid mixture, the same as that utilized to create flat-top patterns, again to remove flat surfaces that were previously covered with SiO<sub>2</sub> and, thus form the pyramidal grains on sapphire. The grain diameter was 3 μm; the spacing between grains was 1 μm.

To prepare the LEDs, metallorganic vapor phase epitaxy was performed in a Taiyo Nippon Sanso SR2000 atmospheric pressure system. For comparison, an LED sample grown on a conventional sapphire (CS) was also prepared. Trimethylgallium, trimethylindium, trimethylaluminum, and ammonia (NH<sub>3</sub>) were used as precursors for Ga, In, Al, and N atoms, respectively. The n- and p-type dopant sources of the nitrides came from silane (SiH<sub>4</sub>) and bis(cyclopentadienyl)magnesium (Cp<sub>2</sub>Mg). First, the sapphire sample was heated at 1180°C in a hydrogen ambient to remove surface contamination. Next, the LED structure was formed; it comprised a 25 nm thick GaN nucleation layer grown at 500°C, a 1.4 μm thick unintentional GaN buffer layer grown at 1130°C, a 3 μm thick Si-doped n-type GaN layer grown at 1130°C, a five-pair multiple quantum well (MQW) layer of In<sub>0.25</sub>Ga<sub>0.75</sub>N/GaN having a thickness of 3/12 nm grown at 795°C, a Mg-doped Al<sub>0.17</sub>Ga<sub>0.83</sub>N/GaN superlat-

\* Electrochemical Society Active Member.

<sup>z</sup> E-mail: rmlin@mail.cgu.edu.tw

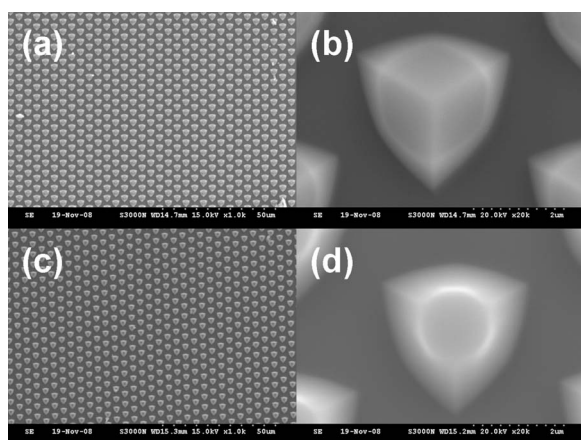


**Figure 1.** SEM images of [(a) and (b)] PPSS and [(c) and (d)] FTPSS before performing epitaxy.

tice grown at 980°C as the electron blocking layer, and a 100 nm thick Mg-doped p-type GaN layer. After epitaxial growth, the samples were heated at 750°C in a N<sub>2</sub> ambient for 20 min to activate the Mg dopants in the p-GaN. The grown wafers were manufactured into devices (295 × 340 μm) using standard photolithography processes. In this paper, the LEDs grown on the CS, PPSS, and FTPSS samples are given the descriptors CS-LED, PPSS-LED, and FTPSS-LED, respectively.

Before performing the epitaxial growth, the surface morphologies of the PPSS and FTPSS were examined using a Hitachi S-3000N scanning electron microscope. A PANalytical X'Pert MRD system was used to inspect the crystalline quality of each sample. The electrical properties, namely, the current–voltage (*I*-*V*) and current–output (*L*-*I*) behavior, were measured using an Agilent B1500A semiconductor device analyzer. A Kimmon IK3501R-G He–Cd laser emitting at 325 nm with a 50 mW output power was used as a photoluminescence pumping source. To perform temperature- and power-dependent photoluminescences, a cryostat cooling with liquid He and neutral density filters with transmittances of 100, 90, 50, 25, 5, and 1% were utilized.

Figure 1a and c displays plan view scanning electron microscopy (SEM) images (1000× magnification) of the PPSS and FTPSS. The grains of both samples were perfectly arranged in hexagonal arrays with an average grain diameter of 3 μm and a uniform grain spacing of 1 μm. Figure 1b presents an SEM image of the grains of the PPSS after performing the wet etching process. The nature of the sapphire crystal makes the etching rate depend on the facet orientation, following the order {0001}(C plane) > {11̄02}(R plane) > {101̄0}(M plane) > {112̄0}(A plane).<sup>9</sup> Because the SiO<sub>2</sub> mask used in this study covered the grain area, the etching began at the surroundings of the mask with the C plane moving downward first during the etching process. As the etching depth increased, the area of the C plane decreased and an inclined facet appeared. The relatively lower etching rates of the other planes caused convex grains composed of {112̄k} facets and having a height of 1.3 μm to form on top of the sapphire. Figure 1d reveals a flat surface on top of an FTPSS grain having a diameter of 1 μm; this flat plane was produced after the first stage of the two-step wet etching method described in the experimental section. The grains of FTPSS, which formed a trapezoid-like shape, featured the same combination of {112̄k} facets as those of the PPSS grains and the flat-top surface.

Figure 2 displays the *I*-*V* characteristic of the LEDs grown on the various substrates. When we examined the CS-LED, PPSS-LED, and FTPSS-LED samples under a forward bias, their forward voltages (*V*<sub>f</sub>) were 2.98, 3.02, and 3.04 V, respectively; i.e., the values of the patterned samples are very close to that of the conventional

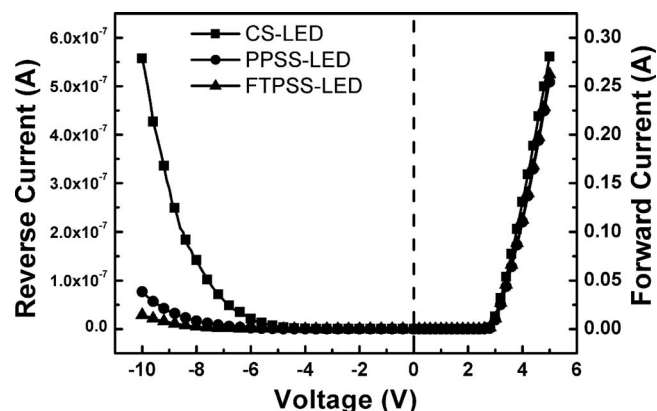


**Figure 2.** *I*-*V* curves of CS-, PPSS-, and FTPSS-LED recorded at room temperature under both forward and reverse biases.

sample and could be even lower after full packaging. Many research groups have demonstrated that the TDD in a device can be reduced by employing a concave-type PSS.<sup>8,10,11</sup> We observed a similar effect in our convex PPSS and FTPSS. To verify this behavior, we also recorded the *I*-*V* curves under a reverse bias (left side of Fig. 2). When we applied a −10 V reverse bias to the samples, the leakage currents of the CS sample, PPSS, and FTPSS were 557, 76.7, and 28.9 nA, respectively. We used identical epitaxy and fabrication conditions to prepare these samples; therefore, we attribute the relatively large leakage current of the CS-LED to many TDs stretching from the sapphire–GaN interface because dislocation is the main cause of leakage. For the PPSS and FTPSS, the leakage current decreased such that we consider the TDDs within these two samples to be restrained. The X-ray diffraction (XRD) spectra in Fig. 3 confirm the improved crystal quality.<sup>12</sup> The full width at half-maximums in the (102) ω scans of the PPSS and FTPSS are very close (360 and 356.4 arcsec, respectively) and are much lower than that in the CS sample (479 arcsec). These values are consistent with our hypothesis of a dislocation suppression effect in the PPSS and FTPSS.

Figure 4 displays the electroluminescence (*L*-*I*) behavior of each of the samples at injection currents varying from 1 to 600 mA applied directly on the chip with a metal heat-dissipating probe station. For each sample, the output intensity increased rapidly upon increasing the injection current from 1 to 200 mA, but increased at a much lower rate thereafter, and finally declined when the injection currents reached 460, 500, and 520 mA for the CS-, PPSS-, and FTPSS-LED,

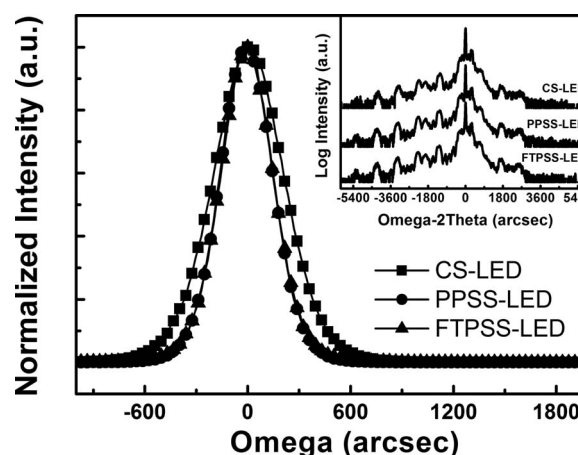


**Figure 3.** High resolution XRD (102) ω scans of CS-, PPSS-, and FTPSS-LED. Inset: Corresponding (002) ω-2θ scans.

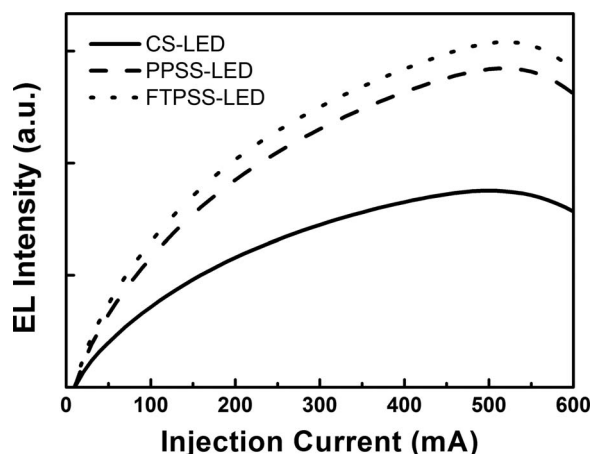


Figure 4. *L-I* profiles of CS-, PPSS-, and FTPSS-LED.

respectively. We attribute this phenomenon to the TDD within the devices. For InGaN blue LEDs, dislocation is considered to be a source of nonradiative recombination centers. When the injection current increases, the junction temperature also rises, and nonradiative recombination becomes stronger because of a phonon effect. As mentioned above, we suspected that the CS-LED had a higher TDD than the other two samples; therefore, its heat effect was strongest, resulting in an earlier output decay. After packing the samples with transistor-outline metal can package and inserting them into an integrating sphere, we found that the CS-, PPSS-, and FTPSS-LED samples had output powers of 5.03, 5.93, and 5.97 mW, respectively, at 20 mA; i.e., relative to that of the CS-LED, the power improved to 17.9 and 18.7% when using the pyramidal and flat-top substrates, respectively. In addition to their improved crystal quality, it is believed that the enhanced output was also due to the higher degrees of interfacial roughness in the patterned samples. When light emitted from an MQW reaches the interface between the patterned substrate and its epilayer, multiscattering can occur to alter the incident angle of light at the air-GaN interface, thereby increasing the probability of light escaping from the device. Furthermore, because the grain shape in the FTPSS was trapezoid-like and more irregular than that in the PPSS, the output from the FTPSS-LED was understandably higher than that from the PPSS-LED.

To further investigate strain characteristics in each sample, a power-dependent photoluminescence spectroscopy was performed at 40 K. Figure 5 displays the emission peak shift of different samples vs pumping power density. To emphasize peak variance, the low power excitation peak wavelengths were set to zero for all samples. As illustrated, all samples performed a blueshift trend in emission wavelength as the pumping power density went higher. The inset of Fig. 3 reveals that the indium contents of these samples were almost identical. The satellite peak positions are quite similar, indicating a strong structural similarity for all three samples, so it is assumed that the difference in blueshift mainly originated from the nature of substrates. For the CS-LED, the value of the peak shift was  $-5.5$  nm while the pumping power density was raised from 1 to  $80$   $\text{W}/\text{cm}^2$ , which is larger than  $-3.46$  and  $-4.46$  nm of PPSS- and FTPSS-LED, respectively. The internal piezoelectric field of nitrides originating from the strain results in a quantum-confined Stark effect (QCSE) and reduces the effective energy gap. While carriers were injected into quantum wells, the charge screening effect occurred and restrained QCSE, which resulted in an emission peak blueshift. Because the CS-LED had the largest power-dependent blueshift among all samples, it was inferred that its QCSE was also the strongest. Wu et al. proposed that air voids can exist upon tilt facets of patterns as a result of growth rate differences of the nitride between flat and inclined facets;<sup>8</sup> Park et al. also observed such voids in a

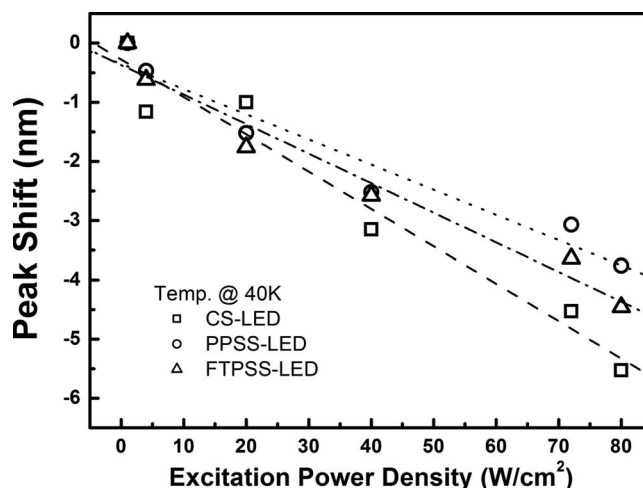


Figure 5. Emission peak shifts vs pumping power density for CS-, PPSS-, and FTPSS-LED. Dashed, dotted, and dashed-dotted lines correspond to their peak-shifting ratio.

semisphere PSS sample.<sup>13</sup> In both studies, the PSS was considered able to alter the strain in LEDs. For the convex patterned samples reported in this work, it was suspected that such kind of strain effect could also occur within the devices. In consideration of surface morphology, the epilayer of the CS-LED is almost fully contacted to the sapphire substrate, which leaves a strong residual strain within quantum wells. Similar to the CS-LED, because the FTPSS-LED has a flat surface on top, its contact area is also larger than the PPSS-LED; thus the emission peak shifted slightly faster as the pumping power went up.

We prepared convex patterned sapphire substrates featuring flat-top and pyramid grains using single and two-step wet etching methods, respectively. The output powers of LEDs incorporating the PPSS and FTPSS were up to 18.7 and 17.9% high, relative to that of the corresponding LED featuring a CS. Meanwhile, the leakage currents also decreased remarkably as a result of lower TDDs. A stronger QCSE was found in the CS-LED and, compared to the PPSS- and FTPSS-LED, indicates a higher residual strain. This shows that a convex patterned sapphire substrate could not only enhance output power of LEDs but also lower residual strain within quantum wells.

Chang Gung University assisted in meeting the publication costs of this article.

## References

1. S. Nakamura, M. Senoh, N. Iwasa, and S. Nagahama, *Jpn. J. Appl. Phys., Part 2*, **34**, L797 (1995).
2. S. Nakamura and G. Fosei, *The Blue Laser Diode*, Springer-Verlag, Berlin (1997).
3. E. F. Schubert, *Light Emitting Diodes*, 1st ed., Cambridge University Press, Cambridge, MA (2003).
4. T. S. Zheleva, O. H. Nam, M. D. Bremser, and R. F. Davis, *Appl. Phys. Lett.*, **71**, 2472 (1997).
5. A. Sakai, H. Sunakawa, and A. Usui, *Appl. Phys. Lett.*, **71**, 2259 (1997).
6. C. H. Chiu, H. H. Yen, C. L. Chao, Z. Y. Li, P. C. Yu, H. C. Kuo, T. C. Lu, S. C. Wang, K. M. Lau, and S. J. Chang, *Appl. Phys. Lett.*, **93**, 081108 (2008).
7. F. Dwikusuma, D. Saulys, and T. F. Kuech, *J. Electrochem. Soc.*, **149**, G603 (2002).
8. D. S. Wu, W. K. Wang, K. S. Wen, S. C. Huang, S. H. Lin, R. H. Horng, Y. S. Yu, and M. H. Pan, *J. Electrochem. Soc.*, **153**, G765 (2006).
9. S. J. Kim, *Jpn. J. Appl. Phys., Part 1*, **44**, 2921 (2005).
10. J. Wang, L. W. Guo, H. Q. Jia, Y. Wang, Z. G. Xing, W. Li, H. Chen, and J. M. Zhou, *J. Electrochem. Soc.*, **153**, C182 (2006).
11. T. V. Cuong, H. S. Cheong, H. G. Kim, H. Y. Kim, C. H. Hong, E. K. Suh, H. K. Cho, and B. H. Kong, *Appl. Phys. Lett.*, **90**, 131107 (2007).
12. B. Heying, X. H. Wu, S. Keller, Y. Li, D. Kapolnek, B. P. Keller, S. P. DenBaars, and J. S. Speck, *Appl. Phys. Lett.*, **68**, 643 (1996).
13. E. H. Park, J. Jang, S. Gupta, I. Ferguson, C. H. Kim, S. K. Jeon, and J. S. Park, *Appl. Phys. Lett.*, **93**, 191103 (2008).